

## Research Article

## Exploring Halophilic Bacteria *Bacillus clausii* Isolated from Madura Salt Pond: Challenges of Utilization in Hypersaline Microbial Fuel Cells for Fish Processing Wastewater Treatment

Marcelinus Christwardana\*

Department of Chemistry, Faculty of Science and Mathematics, Diponegoro University, Semarang, Indonesia  
Master Program of Energy, School of Postgraduate Studies, Diponegoro University, Semarang, Indonesia  
Research Collaboration Center for Electrochemistry, BRIN-UNDIP, Indonesia

Mukhammad Asy'ari and Muhammad Ragil Saputra

Department of Chemistry, Faculty of Science and Mathematics, Diponegoro University, Semarang, Indonesia

H. Hadiyanto

Department of Chemical Engineering, Faculty of Engineering, Diponegoro University, Semarang, Indonesia

\* Corresponding author. E-mail: marcelinus@lecturer.undip.ac.id DOI: 10.14416/j.asep.2025.01.003

Received: 7 September 2024; Revised: 24 October 2024; Accepted: 28 November 2024; Published online: 10 January 2025

© 2024 King Mongkut's University of Technology North Bangkok. All Rights Reserved.

### Abstract

This study investigates the influence of different NaCl concentrations on the performance of halophilic bacterial microbial fuel cells (MFCs) by using *Bacillus clausii*. The electron transfer rate constant ( $k_s$ ) revealed that MFCs operating at 10% NaCl exhibited the highest value of  $2,318 \text{ s}^{-1}$ . The corresponding  $R_s$  and  $R_{ct}$  values for these MFCs were determined to be  $10.19 \Omega$  and  $4.74 \Omega$ , respectively. Remarkably, the maximum power density (MPD) for MFCs at 10% salinity reached  $39.79 \pm 0.22 \text{ mW/m}^2$ , demonstrating a remarkable 33-fold increase compared to MFCs operating without added salinity. Furthermore, the estimated chemical oxygen demand (COD) removal efficiency for fish processing wastewater reached  $95.45 \pm 1.07\%$ , with MPD of  $50.92 \pm 0.28 \text{ mW/m}^2$ . This study underscores the positive impact of salinity on the performance of halophilic bacterial MFCs, offering valuable insights for the optimization of MFC systems in the treatment of saline wastewater, such as fish processing industries.

**Keywords:** Bioenergetic, Bioenergy, Bioresource, Electron transfer, Microbial fuel cell, Wastewater

### 1 Introduction

Fish processing wastewater is notoriously difficult to treat owing to its high organic load and salinity, which may exceed the capacity of standard treatment systems [1]. This kind of wastewater often has proteins, lipids, and other organic substances necessitating sophisticated treatment techniques to avert environmental contamination. Conventional methods inadequately address these situations, resulting in insufficient treatment and possible harm to aquatic ecosystems. A viable alternative is the use of Microbial Fuel Cells (MFCs), which harness the

metabolic processes of microorganisms to clean wastewater while simultaneously generating power [2].

MFCs are a technology that converts microbial activity's chemical energy into electricity via an electrochemical process. MFCs are powered by microorganisms, such as bacteria, which oxidize organic compounds at the anode during anaerobic respiration and release electrons. An electric current flow from the anode to the cathode as a result of the capture of electrons by the anode. At the cathode, electrons from the electric current are used to reduce inorganic compounds, producing an electrochemical

potential that generates electricity. The potential use of MFCs as a renewable energy source is extremely promising. MFCs are capable of producing electricity from organic waste or renewable natural resources [3]. They aid in waste treatment and contribute to the reduction of environmental pollution. MFCs can convert local waste into local energy sources in remote locations. The use of MFCs as a sustainable energy alternative is a step in the right direction towards meeting future energy demands.

One of the candidates used as a biocatalyst in MFCs is halophilic bacteria. As biocatalysts for MFC, halophilic microorganisms have advantages and disadvantages. Its benefits include adaptability and optimal performance in highly saline environments, enabling the use of MFCs in seawater or effluent containing a high salinity [4]. During their metabolism, halophilic bacteria can also decompose complex organic compounds, releasing electrons and protons [5]. To optimize the production of electricity in MFCs, however, it is necessary to surmount disadvantages such as relatively slow reaction rates and electron transfer efficiency [6].

The effect of salinity level in hypersaline conditions on the availability of halophilic bacterial substrates in MFCs is crucial to understanding the efficacy of biocatalysts in salt-rich environments. This is also very important if later the halophilic bacterial MFC system is used to treat wastewater that has high salinity levels or hypersaline. The solubility of organic compounds that are substrates for halophilic microbes can be affected by salinity, which is the total salt concentration in solution [7]. As salinity rises, organic compounds tend to become less soluble, limiting the availability of substrates for halophilic bacteria in MFCs [8]. In addition, the relationship between salinity and ion concentration is extremely significant. Typically, an increase in salinity is accompanied by an increase in the concentration of ions, such as sodium ( $\text{Na}^+$ ), potassium ( $\text{K}^+$ ), and chloride ( $\text{Cl}^-$ ). In MFCs, the presence of these ions can alter the stability of the microbial environment and the biocatalyst's activity. High ion concentrations can affect the electrochemical potential and redox activity at the anode and cathode, which in turn impacts the MFCs' ability to produce electricity [9].

The efficacy of halophilic bacteria in MFCs is significantly influenced by the salinity of the surrounding environment. According to their adaptation requirements, halophilic microbes perform optimally at specific salinity levels [10]. In MFCs, a

salinity that is optimal can improve cell stability, enzymatic activity, and electron transfer efficiency. Toxic effects or growth inhibition can inhibit the performance of halophilic microbes at extremely high or low salinity levels.

Numerous investigations pertaining to halophilic bacteria have been conducted by multiple prior researchers. In their study, Puganzendhi *et al.*, employed Saline Anode – Microbial Fuel Cells (SA-MFCs) as a means to address the treatment of aquaculture wastewater while simultaneously producing bioenergy [11]. The utilization of MFCs for the treatment of seawater sewage, employing *Halomonas* bacteria, was investigated in a study conducted by Liu & Wu [12]. Ghorab *et al.*, employed MFCs as a means to address the treatment of tannery wastewater under saline conditions [13]. The previous study conducted by Gurav *et al.*, investigated the utilization of halophilic *Bacillus circulans* BBL03 as a biocatalyst in MFCs [14]. In a study conducted by Monzon *et al.*, the researchers investigated the impact of quorum sensing autoinducers on the augmentation of biofilm formation and power generation in hypersaline MFCs [15]. Upon examination of the aforementioned studies, it is evident that the halophilic bacteria employed exhibit an outstanding level of variability and diversity. These bacteria can be either single cultures or mixed cultures, derived from anaerobic sludge or similar sources. The favorable conditions presented by saline or hypersaline environments offer a promising avenue for the potential utilization of *B. clausii* as a biocatalyst.

*B. clausii*, as one of the halophilic bacteria, is a preferable candidate for use as a biocatalyst in MFCs due to its distinctive characteristics. *B. clausii* is a Gram positive bacterium with a thick cell wall that provides resistance to the high osmotic pressure that frequently occurs in environments with an excess of salt [16]. In addition, *B. clausii* can create endospores, which are dormant forms that protect cells from harsh environmental conditions and allow them to survive for a long time in unfavorable environments. *B. clausii* possesses robust metabolic capabilities, including the production of specific enzymes that play a role in oxidizing complex organic compounds, in addition to its robust resistance and adaptability [17]. *B. clausii* optimizes the decomposition of organic compounds and enhances electron production during metabolism, making it an effective biocatalyst for MFCs. One species, *B. clausii* J1G-0%B, cultured from a salt pond in Indonesia, exhibits several advantages due to its

origin [18]. These microbes demonstrate stable enzyme activity, leading to consistent microbial activity. Consequently, this bacterium shows high tolerance to elevated salinity levels, making it suitable as a biocatalyst in MFCs for treating hypersaline wastewater.

This research aims to gain an in-depth understanding of the electrochemical characteristics and performance of MFCs that use halophilic bacteria *B. clausii* as biocatalysts at various levels of salinity in hypersaline condition. Based on the extant literature, the utilization of *B. clausii* as a biocatalyst in MFCs, particularly under hypersaline conditions, remains unexplored in prior investigations. The present study purports to establish its novelty within the realm of research. In half-cell conditions, electrochemical properties such as cyclic voltammetry (CV), rate determining step (RDS), and the quest for the electron transfer rate constant are measured. The efficacy of full-cell MFCs is determined by measuring the voltage during incubation and the power density. The results of this study are anticipated to shed new light on the

relationship between salinity and the efficacy of MFCs containing the halophilic bacteria *B. clausii* as biocatalysts. A comprehensive understanding of the electrochemical properties and performance response of MFCs under varying salinity conditions will provide a solid foundation for the development of MFC applications in salt-rich environments. Consequently, this research will make a significant contribution to increasing the potential for the use of sustainable energy sources through MFCs in specific environmental conditions, as well as to a better understanding of halophilic bacteria, particularly *B. clausii*, as biocatalysts in energy and environmental technologies.

## 2 Materials and Method

### 2.1 Preparation of halophilic bacteria

*B. clausii* J1G-0%B, a strain of bacteria, was obtained from a salt pond located in the Madura Island region, as depicted in Figure 1.



**Figure 1:** Location of collecting halophilic bacteria in Madura salt pond, East Java, Indonesia ( $-7.22^{\circ}\text{S}$ ,  $113.21^{\circ}\text{E}$ ).

The isolation of this strain was carried out at the Biochemistry Laboratory, which is part of the Department of Chemistry at Diponegoro University [18]. The strain was subsequently preserved for future utilization. In order to establish a stock culture of *B. clausii* J1G-0%B, a strain isolation procedure was conducted using agar media supplemented with various nutrients. The composition of the agar halophilic media consisted of 0.05 grams of yeast extract, 0.1 grams of tryptone, 0.3 grams of KCl (99.5%), 5 grams of NaCl (99%), 2 grams of MgSO<sub>4</sub> (97%), 0.3 grams of trisodium citrate (99%), 0.036 grams of FeCl<sub>3</sub> (97%), and 1 gram of agar, which all purchased from Sigma Aldrich (St. Louis, Missouri, USA). The aforementioned components were solubilized in a 100 mL volume of de-ionized water. The pH of the solution was carefully adjusted within the range of 7.5–7.8 by employing a NaOH solution (97%). The growth medium was subjected to autoclaving at a temperature of 121 °C for a duration of 15 minutes prior to inoculation. Additionally, it is important to point out that all inoculations were conducted under semi-aerobic conditions. The incubation was then conducted at 27 °C for 72 h.

## 2.2 MFCs setup

The MFCs are comprised of a single chamber electrochemical cell constructed using polyacrylic (Phychemi, China) as the material for the chamber. The chamber is equipped with openings on its sides, through which the cathode electrodes are strategically positioned, where establish direct contact with the surrounding air, as depicted in Figure 2. The anode and cathode utilized in this study are constructed using

commercially plain carbon felt (CF) based on polyacrylonitrile (PAN), without any metal catalyst addition, obtained from KWK Steel Co., Ltd (Zhejiang, China). This carbon felt materials are carefully connected to copper wire in order to establish a reliable electrical connection with the external circuit. The membrane separator employed in this study was Nafion 117. The present study involved the production of MFCs in triplicate, thereby ensuring the replication of experimental conditions. A single colony of the halophilic bacteria *B. clausii* J1G-0%B was aseptically extracted from the stock culture agar using a sterile needle. Subsequently, the loop needle is immersed into a volume of 100 ml of halophilic medium, which possesses the same composition as described in the preceding section, with the exception of agar. The salinity level was modified by altering the concentration of NaCl at three different levels in hypersaline conditions, namely 5%, 10%, 15%, and 20% w/v. Concentrations of NaCl above 20% w/v were not observed, assuming that many cells had already undergone lysis due to the osmotic pressure between the cells and the salt-containing medium. At the commencement of the experiment, a solution comprising of halophilic bacteria and nutrient components was introduced into the MFC reactor. During the incubation operation lasting 72 hours and temperature of 27 °C, the anodes and cathodes of all MFCs were interconnected with a 1000 Ω external load. Additionally, the temperature was maintained at 37 °C throughout the duration of the experiment. In order to conduct control experiments, the anolyte in the MFCs consisted of halophilic bacteria and nutrients, excluding the presence of NaCl.

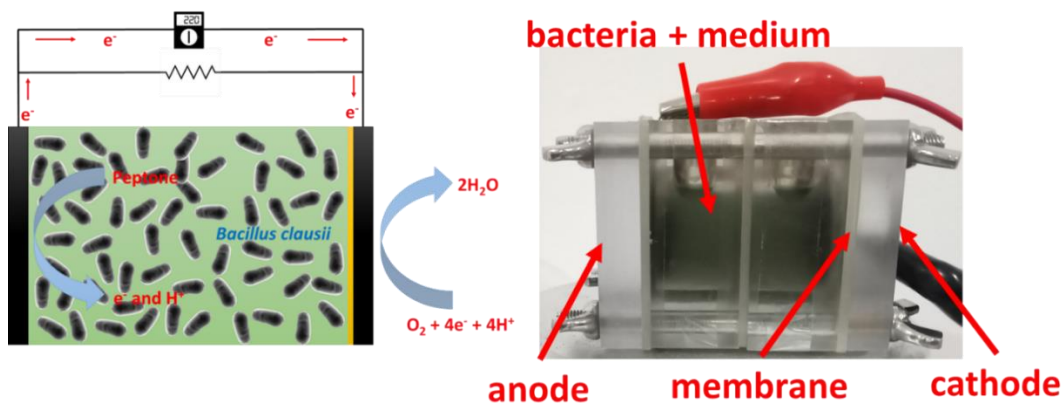


**Figure 2:** Schematic diagram (left) and photograph (right) of MFC reactor.

### 2.3 MFCs electrochemical characterization

The anolyte, which consisted of *B. clausii* J1G-0%B and growing medium, was subjected to half-cell examination to evaluate its composition under different NaCl concentrations. The potentiostat, which is based on Arduino technology, is linked to a computer for the electrochemical measurements. The counter electrode used in this experiment was a Pt wire, the reference electrode utilized was an Ag/AgCl electrode immersed in a 3.0 M KCl solution, while glassy carbon electrodes were used as the working electrodes [19]–[21]. The electrolyte used in this study consisted of a halophilic growing medium supplemented with *B. clausii* J1G-0%B, under controlled atmospheric conditions. Cyclic Voltammetry (CV) was conducted with scan rates ranging from 100 to 1600 mV/s, with a scan window spanning from  $-1$  to  $1$  V vs. Ag/AgCl reference electrode. In order to conduct a test on the performance analysis of single cells, the anolyte was prepared using *B. clausii* J1G-0%B and growth medium containing different concentrations of NaCl. The voltage and power density of microbial fuel cells (MFCs) were then measured to assess their performance. In order to measure the voltage, the MFC reactor is linked to a UNI-T UT61E multimeter and a  $1000\ \Omega$  external load is applied [22], [23]. In the meanwhile, the data collecting equipment consistently observes the output voltage throughout a duration of 72 h. A resistor box (Elenco RS500 Resistance Substitution Box, Illinois, USA) was placed between the anode and cathode of the halophilic bacteria microbial fuel cells (MFCs). The resistor box was adjusted to a range of  $5\ \text{M}\Omega$ – $10\ \Omega$  in order to determine the power density. Simultaneously, a data capture device was used to record the output voltage at 15-minute intervals. The power was determined by using the mathematical expression  $P = V \times I$ , where  $P$  represents the power,  $V$  denotes the potential, and  $I$  means the current density.

### 2.4 Chemical analysis

The growth of the sample was assessed through the quantification of optical density (OD) at a wavelength of 600 nm, employing the LW Scientific UV-200-RS Ultraviolet and Visible Spectrophotometer (Georgia, United States). The pH and oxidation-reduction potential (ORP) were quantified utilizing an advanced digital 4 in 1 water quality sensor YY-400

(Guangdong, China). The morphology of the anode, to which halophilic bacteria were attached during the incubation period, was examined utilizing the Scanning Electron Microscope JEOL JSM-6510LA (Tokyo, Japan). Total Dissolve Solid (TDS) and electroconductivity (EC) were measured by using 2 in 1 TDS-EC meter. The assessment of chemical oxygen demand (COD) was conducted using HANNA COD tube tests HI93754A-25, which had a measuring range spanning from 0 to 15,000 mg/L. The examination consisted of a two-hour chemical digestion procedure conducted at a temperature of  $150\ ^\circ\text{C}$  using a HANNA Instruments HI 839800 digester. Following the completion of the digestion procedure, the samples were permitted to undergo a cooling phase, after which they were subjected to analysis using a HANNA Instruments HI 83099 photometer.

### 2.5 Statistical analysis

The experiments were conducted in triplicate to ensure the reliability and reproducibility of the results. Data obtained from these experiments were subjected to statistical analysis, where the mean and standard deviation were calculated. The results are presented as the mean  $\pm$  standard deviation, providing a measure of central tendency and variability. This approach allows for a comprehensive understanding of the data distribution and the precision of the measurements.

## 3 Results and Discussion

### 3.1 Electrochemical analysis

#### 3.1.1 Half-cell analysis

Figure 3(a) depicts a maximum at a reduction potential of  $-0.75$  V vs. Ag/AgCl on days 0 and 3. Since the incubation was conducted in a semi-aerobic environment, this peak is likely due to the reduction of  $\text{NAD}^+$  to NADH. No oxidation peaks were detected, which may be due to halophilic bacteria's loss of salt adaptation, perturbed cell osmotic balance, inefficient organelle function, and impaired nutrient uptake [24]. This metabolic disorder affects a number of oxidation reactions, including the formation of  $\text{CO}_2$  and ammonia, as well as the activity of enzymes including SOD, catalase, and peroxidase [25]. However, the upward shift of the electrical double layer from 0 V vs. Ag/AgCl proves that there is an oxidation process of organic matter by halophilic bacteria. Figure 3(b)

illustrates the appearance of a minor peak at 0.17 V vs. Ag/AgCl. This peak is attributed to the oxidation of Cytochrome c ( $\text{Fe}^{2+}$ ) to Cytochrome c ( $\text{Fe}^{3+}$ ) and the release of electrons in the electron transport chain process during metabolism. On the other side, Vijay *et al.*, said that the oxidation peak represents the oxidation of carbon source (in this case tryptone) to  $\text{CO}_2$  as a result of metabolic processes [26]. In environments containing 5% salt, there were no issues with osmotic stress, cellular function, nutrient absorption, or adaptation of halophilic microorganisms. As a consequence, the *B. clausii* bacteria's metabolism runs smoothly, and the electrodes capture more protons and electrons. The reduction peak was also observed at around 0.6 V vs. Ag/AgCl, which is thought to be affected by the decrease in pH value under these conditions [27]. The peak represents a reduction in

NAD<sup>+</sup> that overlaps with the ORR marginally. Figure 3(c) depicts the visible oxidation peak at 0.1 V vs. Ag/AgCl. This indicates that under conditions of 10% NaCl, *B. clausii* bacteria have an excellent metabolic rate. This healthy metabolism reduces osmotic stress in bacteria, increases the efficacy of organelle function, minimizes disruption of nutrient absorption, and preserves bacteria's salt adaptation [28]. The efficacy of enzymes such as catalase, superoxide dismutase, and peroxidase in catalyzing reduction and oxidation reactions in halophilic bacterial cells is also influenced by the efficient operation of organelles. Despite the success of the oxidation reaction, the apex of the reduction reaction was slightly diminished relative to the 5% NaCl condition. This demonstrates that the salt concentration can influence the predominant type of reaction, both reduction and oxidation.

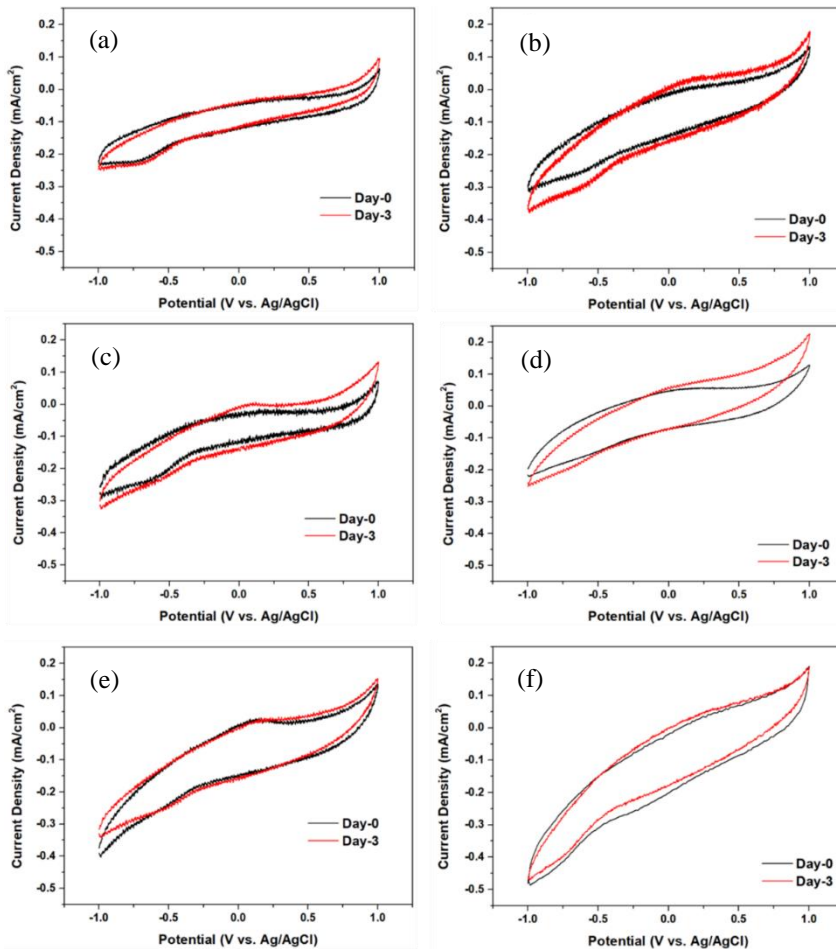


**Figure 3:** CV of halophilic *B. clausii* bacteria culture before and after incubation process with NaCl concentration of (a) 0, (b) 5, (c) 10, and (d) 15, and (e) 20%. While, (f) is CV curves of medium only as a negative control.



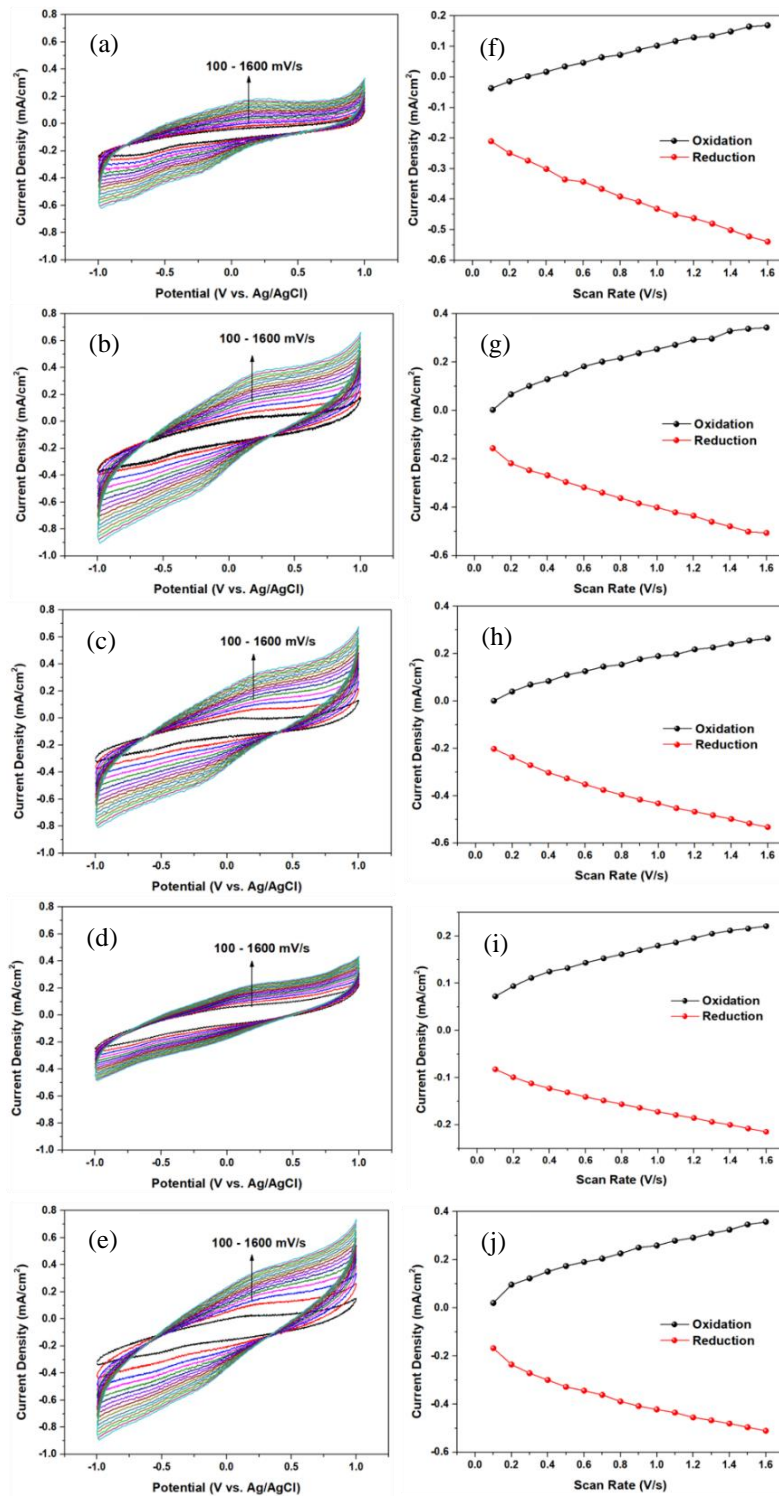


**Figure 4:** CV of halophilic *B. clausii* bacteria culture after an incubation process with NaCl concentration of (a) 0, (b) 5, (c) 10, and (d) 15%, and (e) 20% with various scan rate from 100 to 1600 mV/s. While, (f)–(j) is its relationship between scan rate and peak current density.



Figures 4(a)–(e) depict the CVs of halophilic MFCs with salinity variations at different scan rates. As a preliminary stage in determining the Rate Determining Stage (RDS) and deriving the Electron Transfer Rate Constant ( $k_s$ ), this analysis was conducted. The value of the electrical double layer and the redox peaks increases as the scan rate increases, as evidenced by the four images. In addition, it was discovered that oxidation peaks were still visible at high scan rates in all four images, although the oxidation peaks at 20% NaCl concentration were not as distinct as those at 0%, 5%, 15%, and 20%. Some *B. clausii* cells may have perished because they were in an environment with extremely high salinity, which inhibited redox reactions in metabolic processes. In contrast, in the reduction portion, the peak at a potential of  $-0.6$  to  $-0.75$  V vs. Ag/AgCl that appears at a low scan rate diminishes at a high scan rate. However, this was accompanied by a more pronounced ORR peak at  $-0.25$  V vs. Ag/AgCl, where the peak is more pronounced at a high scan rate than at a low scan rate. The occurrence of peaks that are either diminishing in prominence or becoming more visible can be attributed to a multitude of factors. The attainment of equilibrium in redox reactions necessitates different durations of time, depending on the specific reaction under consideration. Reactions characterized by a longer equilibration time may not be able to achieve equilibrium within a short time frame, such as when a high scan rate is employed. Consequently, the redox peaks associated with these reactions may exhibit a decrease in magnitude or even vanish altogether under such conditions. Secondly, it is worth noting that the observed phenomenon can be attributed to peak broadening. Peak broadening refers to the phenomenon where the width of a peak increases when the scan rate is high, consequently leading to a decrease in the intensity of the three peaks [30]. Thirdly, it is worth noting that the insufficient mass imbalance observed at the electrode surface can lead to a diffusion-limited reaction [31]. The observed phenomenon results in a modulation of the intensity of the redox peaks, which may either diminish or amplify. The comprehension of the Rate Determining Step (RDS) plays a crucial role in enhancing the development and fabrication of electrodes and biocatalysts with improved efficiency for MFCs. Through the identification of the reaction stages that impose limitations on the rate of progress, it becomes possible to strategically optimize the properties and characteristics of both the electrode and biocatalyst.

This optimization process aims to enhance the performance and reaction rate of the MFCs. The figures presented in Figure 4(f)–(j) demonstrate a clear depiction of a nonlinear correlation between scan rate and current density. This observation suggests that the diffusion reactions play a crucial role in constraining all redox reactions that take place during the incubation of halophilic bacteria at different salinity levels. Microbial activity takes place at the interface where the microorganism and the electrode surface come into contact. The accumulation of metabolic reaction products at the surface of the electrode leads to the establishment of a concentration gradient. The gradual buildup of substances over a period of time leads to the formation of a diffusion barrier, which hinders the movement of reactants toward the surface of the electrode and consequently obstructs the efficient transfer of electrons [32]. The internal resistance of microbial fuel cells often exhibits a relatively high magnitude, leading to a notable decrease in voltage, especially during the flow of current. This phenomenon can have a constraining effect on the overall reaction rate within the system [33].

The value of the electron transfer rate constant ( $k_s$ ) at various concentrations of NaCl in a microbial fuel cell containing the halophilic bacterium *B. clausii* was determined using Laviron curves [34], as shown in Figure 5(a)–(e). The highest  $k_s$  values were observed at a 10% NaCl concentration with values of  $2.318 \pm 0.037$  s<sup>-1</sup>, followed by 15%, 5%, 20%, and 0% NaCl concentrations with  $k_s$  values of  $1.552 \pm 0.081$ ,  $1.440 \pm 0.024$ ,  $0.765 \pm 0.045$ , and  $0.014 \pm 0.001$  s<sup>-1</sup>, respectively. This result is consistent with the findings of CV analysis, which demonstrated that the redox peaks in *B. clausii* were greatest at 10% NaCl concentration, followed by 15% and 5% concentrations. A high value for  $k_s$  indicates that the electron transfer reaction or redox reaction occurs rapidly. The high value of  $k_s$  indicates that electrons can be transferred readily from the electrode to the reactant species or vice versa, allowing the redox reaction to occur rapidly and effectively. A high concentration of NaCl as an electrolyte can speed up the rate of electron transfer. However, too high concentration of NaCl can kill halophilic microbes and reduce the rate of electron transfer owing to diffusion barriers at high salt concentrations. Concentrated electrolyte solutions also tend to have high ion densities, which can result in mutual repulsion between these ions, reducing ion mobility and



inhibiting diffusion rates. With a high  $k_s$  value at a 10% NaCl concentration, it can be concluded that the halophilic bacteria *B. clausii* is capable of carrying out redox reactions promptly, generating higher electric currents, and enhancing the overall performance of microbial fuel cells under these conditions. The

comparison of  $k_s$  value from all samples and its correlation with NaCl concentration can be seen in Figure 5(f), where the value of  $R^2$  is 0.988. The relationship between NaCl concentration and  $k_s$  is modeled as a parabola, it suggests a quadratic relationship.

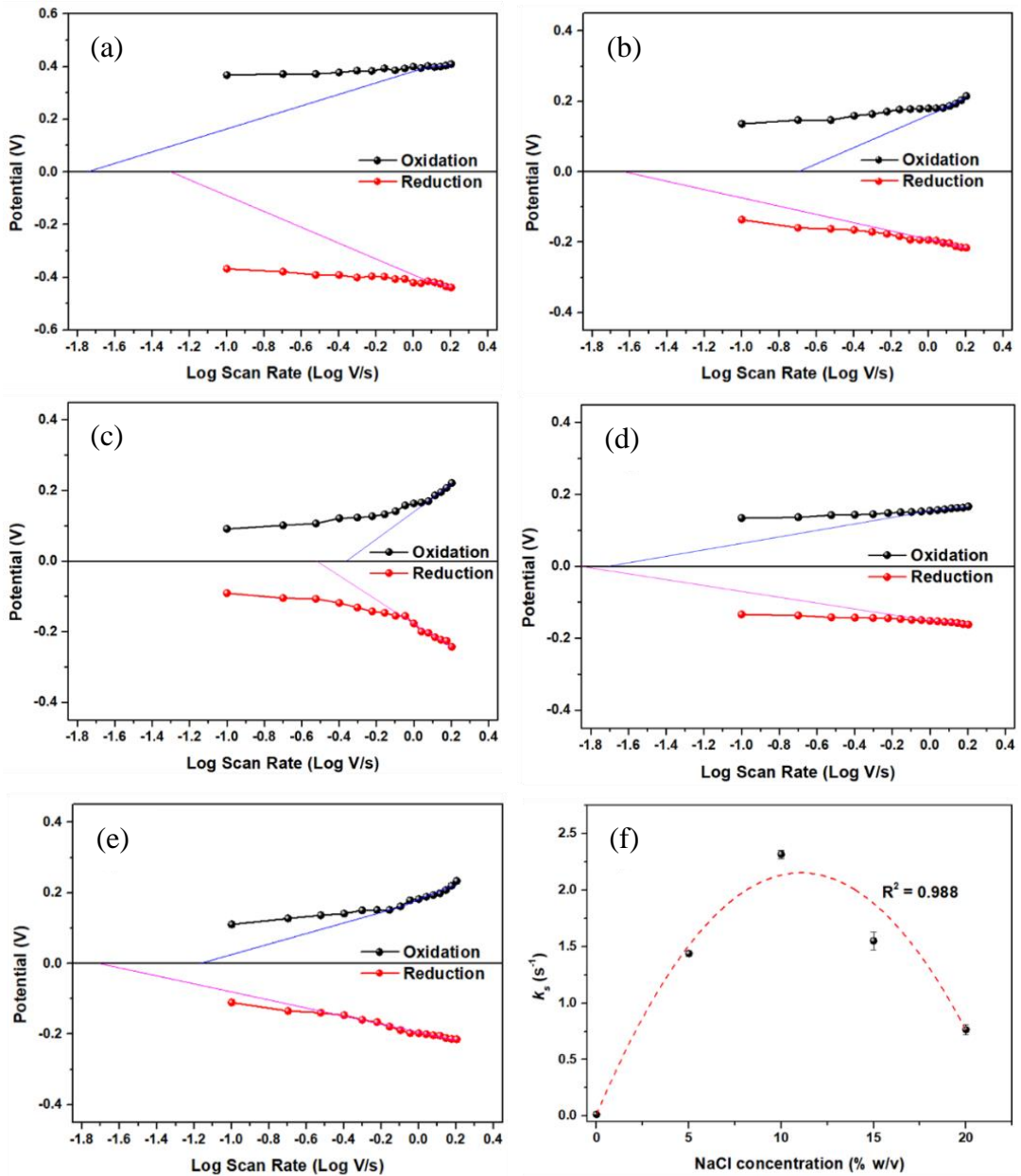


**Figure 5:** Laviron curves of halophilic *B. clausii* bacteria culture after an incubation process with NaCl concentration of (a) 0, (b) 5, (c) 10, (d) 15%, and (e) 20%. While, (f) is the correlation between  $k_s$  value and NaCl concentration.

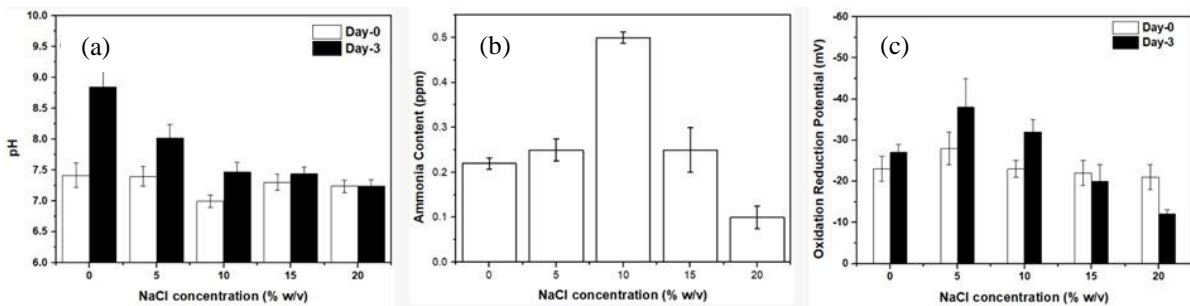


**Figure 6:** (a) pH, (b) ammonia, and (c) ORP level of halophilic *B. clausii* bacteria culture during incubation process.

In order to ascertain the quantitative validity of the  $k_s$  values obtained in this research, it is necessary to conduct a comparative analysis with the  $k_s$  values reported in prior investigations. Table 1 displays a comparative analysis of  $k_s$  values in relation to prior research on MFCs [35]–[40]. Based on the data shown in the table, it can be seen that a significant majority of the anodes used in earlier research on MFC systems were carbon electrodes that underwent some kind of modification. Similar occurrences were seen with the biocatalyst used, mostly with a mixed culture. In this particular investigation, the anode used consisted of carbon felt without any modifications, while the biocatalyst employed was a single culture. Notably, no exogenous mediators were utilized in the experimental setup. This research demonstrates the superiority of the *B. clausii* J1G-0%B strain due to its production of a  $k_s$  value that is equivalent to or larger than that seen in previous comparative studies. Therefore, it is very plausible to consider this strain as a potential biocatalyst for MFCs operating under hypersaline conditions.

Changes in pH were recorded during the three-day incubation of *B. clausii* as shown in Figure 6(a). In the pH analysis, there are two key observations. Firstly, in general, the pH increases after the incubation process. This is due to *B. clausii* consuming tryptone during incubation, with ammonia being one

of the byproducts. Ammonia, being basic, raises the pH of the incubation medium. Secondly, the higher the concentration of NaCl added, the smaller the increase in pH. This is because a higher amount of NaCl results in more water interacting or binding with NaCl, leaving less water available to interact or bind with ammonia to form ammonium hydroxide. Consequently, the ionization of ammonium hydroxide is limited, resulting in a less significant pH change. Conversely, when no NaCl or a lower concentration of NaCl is added, the ammonia produced from bacterial metabolism interacts with water to form ammonium hydroxide, which ionizes easily and significantly increases the pH. *B. clausii* is capable of producing byproducts such as ammonia ( $\text{NH}_3$ ), which is alkaline by nature and can raise the pH of a solution [41]. Production of ammonia can be shown in Figure 6(b). Increased ammonia production during incubation may be one of the causes of the elevated pH. During the bacterial growth process, metabolites and byproducts are emitted, which can alter the pH of the surrounding environment [42]. Bacteria consume nutrients and produce new compounds that can alter the pH of their surroundings. The marginal rise in pH attributed to *B. clausii* metabolic activity is believed to stem from the excretion of organic acids, despite the alkaline ammonia generated concurrently.

**Table 1:** Comparison of  $k_s$  value with previous studies.

Anode Material	Anode Biocatalyst	Electrolyte	$k_s$ ( $\text{s}^{-1}$ )	Ref.
CNT hydrogel-modified carbon paper carbon felt	mixed culture (from anaerobic sludge)	PBS pH 7.0	0.1	[35]
TNA- $\text{H}_2$	mixed culture ( <i>Trichoderma harzianum</i> and <i>Pseudomonas fluorescens</i> )	5mM solution of Fe(III)/Fe(II) in 0.1 M $\text{KNO}_3$	2.97	[36]
PPy-CMC-TiN/CB	mixed culture (fresh anodic effluent from an existing parent MFC reactor)	M9 medium with 1 g/L sodium acetate nutrient buffer solution	2.38	[37]
3D Graphene GNP/CNT/CPE carbon felt	mixed culture (from activated sludge and other successfully domesticated strains in microbial reactors)		0.59	[38]
	<i>Shewanella oneidensis</i> MR-1	<i>Shewanella</i> nutrient	0.0176	[39]
	mixed culture (from domestic wastewater)	YPD medium	1.56	[40]
	<i>B. clausii</i> J1G-0%B	halophilic medium in PBS	2.318	this work

After incubation, the Oxidation-Reduction Potential (ORP) becomes negative and shows a tendency of reduction compared to the oxidation reaction during *B. clausii* incubation (Figure 6(c)). A negative ORP for anode biocatalyst indicates an oxidation tendency, while a more positive ORP indicates a reduction tendency. Lower anode ORP is preferable, means, signifies increased electron generation. During incubation, bacteria such as *B. clausii* might oxidize organic compounds present in the growth medium to simpler compounds such as CO<sub>2</sub> and H<sub>2</sub>O. ORP changes to negative can also occur due to chemical interactions in the incubation environment or changes in the concentration of organic compounds or reactants in solution [43]. Chemical reactions involving oxidative and reductive compounds can alter the system's equilibrium of redox reactions. Changes in the concentration of reductive compounds or reactants within the growth medium can also affect ORP values [44].

### 3.1.2 Full-Cell analysis

The study included the characterization of the half cells of halophilic bacterial microbial fuel cell (MFC) biocatalysts at varying salinity levels. Subsequently, the performance of MFCs using these halophilic bacterial biocatalysts at various salinity levels was examined by measuring the closed-circuit voltage (CCV) and its associated polarization curve. The first assessment included measuring the impact of time on the CCV of all MFCs, with the corresponding findings shown in Figure 7(a). The figure illustrates a clear correspondence between the trend in CCV and the pattern of bacterial growth, characterized by several phases including lag, log, stationary, and death phases. This observation suggests that the growth phase of halophilic bacteria has an indirect impact on the generation of protons and electrons through redox reactions inside the cell's metabolic pathways.

In this research, a comprehensive analysis was conducted to investigate the influence of varying NaCl concentrations, specifically sodium chloride salt, on the performance of Microbial Fuel Cells (MFCs). The results unveiled pronounced disparities in the growth dynamics of microorganisms within MFCs exposed to different NaCl concentrations. In the case of MFC with 0% NaCl, the prolonged lag phase, spanning approximately 48 h, could be attributed to the time required for microorganisms to adapt to an environment devoid of NaCl. This initial adaptation

process aligned with the delayed onset of the log phase, which commenced after 48 hours, eventually culminating at the 70-hour mark, followed by the stationary phase. In contrast, MFC with NaCl 5% exhibited an exceedingly brief lag phase, indicative of the rapid adaptability of microorganisms to the 5% NaCl environment. However, the swift transition to a stationary phase, which was in turn followed by a marked voltage drop, signifying cell death, hinted at the depletion of available nutrients. This depletion rendered the microbes unable to metabolize efficiently to produce electrons. An MFC with 10% NaCl concentration yielded a robust and consistent log phase, possibly a result of the microorganisms' adaptation to this 10% NaCl concentration. The improved performance in subsequent cycles suggested that the microorganisms had become more efficient in metabolizing the available substrates within the NaCl-enriched environment. Conversely, 15% MFC-NaCl displayed a marginally longer lag phase compared to the 10% NaCl scenario, with a truncated log phase and rapid cell death. The reduced duration of the log phase indicated that a higher NaCl concentration (15%) could impede microorganism growth, likely due to increased salt toxicity inhibiting efficient substrate metabolism. Both MFC with NaCl 5% and 15% experienced a phase of cell death after the stationary phase, resulting in a voltage decline. This underlined the adverse effects of higher salt concentrations on microorganisms and demonstrated that cell death occurred more rapidly at 20% NaCl than at 5% or 15% NaCl. The disparities in the duration of each growth phase could be attributed to the varying levels of microorganism adaptation to different NaCl concentrations and the impact of salt toxicity. The noteworthy voltage drops in MFC with NaCl 5%, 15%, and 20% emphasized how elevated salt concentrations can hinder microorganism growth and activity within MFCs. In contrast, the strong and efficient log phase in MFC with NaCl 10% indicated that the microorganisms had acclimated successfully to higher salt conditions from prior cycles.

The CCV for the halophilic bacteria MFCs at a NaCl concentration of 10% exhibited the greatest value. The average CCV values for the halophilic bacteria MFC at NaCl concentrations of 0%, 5%, 10%, 15% and 20% were  $11.69 \pm 2.28$ ,  $28.89 \pm 13.71$ ,  $154.80 \pm 9.02$ ,  $82.12 \pm 5.76$ , and  $76.98 \pm 1.73$  mV, respectively. Based on the data provided, it is evident that the CCV of MFCs exhibits an upward trend as the salinity level rises, reaching its peak at 10% NaCl

concentration. However, after this point, the CCV experiences a decline as the NaCl concentration further increases to 20%. The findings of this study suggest that salinity has a significant impact on the generation of electricity in the MFCs. The observed rise in the CCV value up to 10% salinity circumstances indicates a more favorable environment for the electrogenic activity of halophilic bacteria. Halophilic bacteria are recognized for their capacity to acclimate to exceedingly saline environments; nonetheless, excessively elevated salt concentrations may also disrupt the intracellular homeostasis of these microorganisms. The observed rise in CCV when exposed to a NaCl concentration of 10% suggests that halophilic bacteria may attain an ideal state of metabolic activity at this particular salinity level. Consequently, a considerable number of electrons produced by the halophilic bacterium *B. clausii* are promptly sent to the electrode via this interaction. Additionally, the augmentation of salinity also leads to a heightened facilitation of electron transport from bacteria to electrodes, as a result of the concurrent elevation in their electrolytic characteristics [45]. Nevertheless, the observed reduction in CCV when exposed to a NaCl concentration of 20% suggests that bacteria have a specific threshold for tolerating elevated salt levels, hence impeding their metabolic processes. These circumstances have the potential to impede cellular activities, such as redox reactions that play a crucial role in the generation of protons and electrons. Furthermore, an excessive presence of osmotic effects has the potential to disturb the equilibrium of cellular water, hence diminishing the proton potential necessary for the generation of energy [46].

The measurement of the maximum power density (MPD) of the halophilic MFCs was also conducted using the polarization and power curves, as shown in Figure 7(b) and (c). The obtained polarization curves demonstrate a positive correlation between the open circuit voltage (OCV) value of MFCs and the concentration of NaCl. The enhanced conductivity of the solution may be attributed to the presence of NaCl in the electrolyte. Enhanced conductivity in the electrolyte facilitates improved transport of ions and electrons. The aforementioned phenomenon might lead to an increased OCV as a consequence of enhanced ion mobility inside the cell. Activation losses are shown to be high when the concentration of NaCl is at 0% and 5%. This is attributed to the fact that at very low NaCl

concentrations, the electrolyte exhibits a correspondingly low level of conductivity. The outcome of this phenomenon is the manifestation of elevated resistance inside the MFCs, which encompasses the presence of activation resistance. Nevertheless, when the concentration of NaCl was increased to 10% and beyond, there was a discernible reduction in activation losses, although the drop was not statistically significant. The augmentation of NaCl concentrations has the potential to hinder the decline in activation losses due to the substantial rise in electrolyte conductivity. This, in turn, leads to a reduction in activation resistance and a notable enhancement in the performance of MFCs. The impact of high NaCl concentrations on ohmic losses is noteworthy since NaCl concentrations beyond 10% have been seen to impede a significant reduction in ohmic losses. The presence of  $\text{Na}^+$  and  $\text{Cl}^-$  ions in the electrolyte is responsible for their function as ion conductors. With increasing amounts of NaCl, there is a corresponding rise in the concentration of ions within the solution. The reduction of ion resistance in the electrolyte leads to a subsequent decrease in ohmic resistance. The presence of a low ion barrier facilitates enhanced ion conductivity inside the MFCs system. Nevertheless, the rise in NaCl levels did not result in any substantial alteration in mass transfer losses. The maximum power density (MPD) of the halophilic bacterial MFC operating at a salinity of 10% was measured to be  $39.79 \pm 0.22 \text{ mW/m}^2$ . In comparison, the MPD values for the halophilic bacterial MFCs operating at salinities of 0%, 5%, 15%, and 20% were determined to be  $1.19 \pm 0.07$ ,  $4.13 \pm 0.16$ ,  $7.70 \pm 0.05$ , and  $2.25 \pm 0.01 \text{ mW/m}^2$ , respectively. The performance of MFC rises by 33 times (3193%) in a short amount of time when the NaCl concentration is increased from 0 to 10%, reducing startup time significantly. It is important to note that our MFC testing did not consider any mediators or media substitutes. This implies that our system was able to produce a significant rise in MPD during a brief startup period of 72 h, using a 10% salinity solution. Furthermore, the observed outcomes were found to be comparable or superior to those reported in previous research endeavors. The comparative analysis of MPD was conducted on MFCs using *B. clausii* as a biocatalyst, and the findings were juxtaposed with the results of other MFCs conducted under saline circumstances, as shown in Table 2 [47]–[51]. The MPD observed in this study has a comparable level to previous studies, as seen by the data presented in the

table. The superior performance observed in other studies can be attributed to the utilization of high-cost Pt/C cathodes and ferricyanide catholytes, which are known to enhance the overall efficiency of the system compared to the materials used in this work. In this work, *B. clausii* used amino acids present in yeast extract and tryptone as a source of carbon. It is known that amino acids undergo a lengthier digestion period inside the metabolic process. Amino acids exhibit a high degree of complexity and diversity. The process of amino acid catabolism involves the conversion of each specific kind of amino acid into a metabolically usable form that may be incorporated into the cellular metabolic pathways. These contribute to the comparatively poor performance of the MPD in this investigation.

The investigation of the correlation between internal resistance and maximum power density in MFCs constitutes a pivotal facet in the assessment of MFC effectiveness. Internal resistance in MFCs is a result of multiple factors originating from within the system. These factors include the interface between the electrode and electrolyte, the biofilm formed by electroactive bacteria, and the electrolyte solution present in the MFC. The presence of a barrier hinders the smooth movement of electrons produced during microbial metabolism from the anode to the cathode, thereby impacting the power generation capacity of the MFCs. The relationship between internal resistance and maximum power density is inversely proportional. As the internal resistance of a system increases, it is observed that the voltage drop across the internal resistance also exhibits a corresponding increase. The internal resistance of halophilic MFCs with NaCl concentrations of 0, 5, 10, 15%, and 20% were 181, 177, 164, 253, and 321  $\Omega$ . The observed phenomenon results in a reduction of the overall voltage potential that can be harnessed for power generation purposes. Consequently, the microbial fuel cell's capacity to generate electrical power experiences a decline. Hence, the optimization of internal resistance holds paramount importance in the pursuit of attaining elevated power densities within MFCs. The optimization of electrode materials, biofilm development, and electrolyte composition are frequently investigated by researchers as potential strategies to mitigate internal resistance.

The complex interaction between internal resistance and salinity levels in MFCs manifests itself in various significant manners. The performance of MFCs is notably affected by salinity, primarily owing

to its direct influence on the ionic conductivity present within the electrolyte. Increased salinity has the potential to initially increase the mobility of ions, which in turn may enhance the rates of electron transfer. Nevertheless, it is worth noting that as the salinity levels progressively increase, a critical threshold is eventually surpassed, leading to a notable upsurge in the internal resistance phenomenon, as shown in Figure 7(d). The observed phenomenon can be attributed to the paradoxical effect arising from the presence of excessively elevated salinity levels [52]. Such conditions have the potential to interfere with the overall structural stability of the biofilm, thereby impeding its conductivity and hindering the efficient transfer of electrons within the biofilm matrix. Furthermore, it is worth noting that the presence of high salinity at the electrode-electrolyte interface has the potential to alter the properties of the electrode surface [53], [54]. This phenomenon frequently results in an augmentation of the charge transfer resistance [55]. As a result, the process of fine-tuning the salinity balance in MFCs can be considered an intricate endeavor aimed at attaining the most favorable circumstances for facilitating efficient ionic and electronic transport within the system. The successful implementation of MFCs in saline environments necessitates the careful selection or modification of salt-tolerant microbial species, the development of appropriate electrode materials, and the precise regulation of operational parameters. These measures are crucial to fully exploit the capabilities of MFCs in saline environments, enabling their effective utilization in applications such as wastewater treatment.

In addition to scrutinizing the performance measurements of MFCs, an assessment was conducted on the performance of *B. clausii* as an anode biocatalyst under different NaCl concentrations. This evaluation was carried out in complete cells utilizing electrochemical impedance spectroscopy (EIS). The Nyquist plot in Figure 7(e) showcases the raw data alongside an equivalent Randles circuit. The parameter denoted as solution resistant ( $R_s$ ) in this context represents the resistance that arises from the interaction between the electrolyte solution and the surface of the electrode. On the other hand, charge transfer resistance ( $R_{ct}$ ) signifies the resistance associated with the bacteria's ability to transfer electrons.  $C_{dl}$ , another parameter of interest, refers to the electric charge that is stored and aligned within the electrochemical system, specifically between the

electrode and the electrolyte. Lastly, the parameter  $W$  pertains to the Warburg diffusion of the element under investigation. The influence of the concentration of NaCl in the electrolyte on the values of  $R_s$  and  $R_{ct}$  in MFCs is of considerable importance. This is primarily attributed to the effect of NaCl concentration on the ionic conductivity and electron transfer processes within the MFC system. The observed figure illustrates a clear correlation between the rise in NaCl concentration and the decrease in  $R_s$  value. The  $R_s$  value of MFCs with varying NaCl concentrations, specifically 0%, 5%, 10%, 15%, and 20% were measured and found to be 10.74, 10.44, 10.19, 10.07, and 9.79  $\Omega$ , respectively. NaCl exhibits electrolytic properties. Consequently, it has the ability to enhance the conductivity of a solution. As the concentration of NaCl increases, the ionic conductivity of the solution also experiences a corresponding increase. The initial augmentation of the solution's ion and electron conductivity enhances its capacity to facilitate charge transfer. Consequently, this leads to a reduction in the  $R_s$  value, thereby amplifying the efficiency of charge transfer between the electrodes and microorganisms within MFCs. The observed figure also demonstrates a notable inverse relationship between the value of  $R_{ct}$  and the concentration of NaCl. At a specific point, it has been observed that the  $R_{ct}$  value exhibits an upward trend as the NaCl concentration reaches a state of excessive concentration. The observed phenomenon can be attributed to the increased density of ions within the solution, which consequently possesses the ability to impede the movement of electrons. The  $R_{ct}$  of MFCs with varying concentrations of NaCl at 0%, 5%, 10%, 15%, and 20% were measured and found to be 7.5, 7.24, 4.74, 7.76, and 8.21  $\Omega$ , respectively. The observed low impedance of the anode suggests that a

significant portion of the electrons generated by the bacteria are efficiently transferred to this modified anode, which functions as an electrical generator. The impact of elevated salinity levels on the properties of electrode surfaces has been observed to result in a decrease in resistance between the electrode and the biofilm formed by microorganisms.

The value of internal resistance is precisely proportional to the value of  $R_{ct}$  as shown in Figure 7(f). The relationship between internal resistance and  $R_{ct}$  is highly interconnected ( $R^2$  is 0.91), with one factor exerting impact on the other. A high internal resistance may lead to an increase in electrochemical potential throughout the MFCs, including at the interface between the electrode and the biofilm [56]. Consequently, this has the potential to increase the value of  $R_{ct}$ . Put simply, when the internal resistance rises, the electrochemical potentials that take place at the electrode and the biofilm become more discernible, leading to an increase in charge transfer resistance at the interface [57]. A possible strategy for mitigating the resistance in the system is to minimize the internal resistance, hence leading to a reduction in the electrochemical potential difference between the electrode and the biofilm. Consequently, this drop in potential difference contributes to a reduction in the  $R_{ct}$ . Hence, in order to enhance the efficiency of MFCs, it is essential to undertake measures aimed at diminishing internal resistance via the careful selection of highly conductive electrodes and the optimization of biofilm composition. The enhancement of electrochemical charge transfer efficiency is crucial in order to boost the output power of MFCs, achieved by minimizing the internal resistance.

**Table 2:** Comparison of MPD value with previous saline MFC studies.

Biocatalyst	Anode	Anolyte	Cathode	Catholyte	MPD (mW/m <sup>2</sup> )	Ref.
<i>Bacillus circulans</i> BBL03	carbon felt	natural seawater and shrimp chitin	Pt/C	50 mM ferricyanide	17.42 (1.742 mW/cm <sup>2</sup> )	[47]
<i>Bacillus cereus</i>	Fe <sub>2</sub> TiO <sub>5</sub> composite-mild steel	1 mM sucrose	SS-304	50 mM potassium ferricyanide	400	[48]
<i>Bacillus subtilis</i>	carbon cloth	M9 medium	Pt/carbon paper	sterilized M9 medium without glucose	10.5 (1.05 mW/cm <sup>2</sup> )	[49]
<i>Bacillus velezensis</i>	aluminium	sterilized nutrient broth	aluminium	sterilized nutrient broth	43.3 (4.33 $\mu$ W/cm <sup>2</sup> )	[50]
<i>Bacillus altitudinis</i> AC11.2	carbon fibers	glucose 0.1 M, thioglycollate 0.5% w/v, and phosphate buffer 0.1 M	carbon fibers	KMnO <sub>4</sub> 0.01 M and phosphate buffer 0.1 M	67.11	[51]
<i>B. clausii</i> J1G-0%B	carbon felt	halophilic medium in PBS	carbon felt	air cathode	39.79	This work



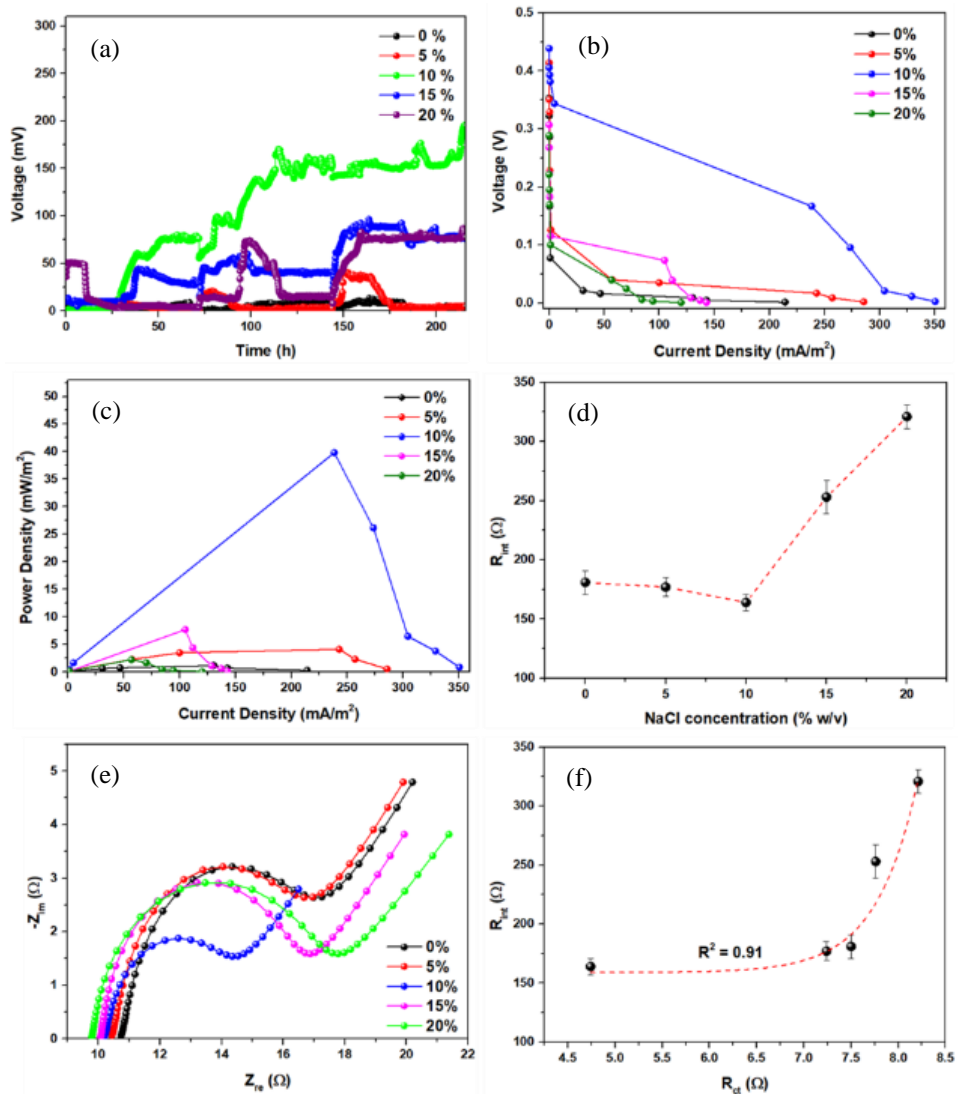


**Figure 7:** (a) Voltage and (b) polarization and (c) power curves of halophilic bacteria MFCs in NaCl levels of 0%, 5%, 10%, 15%, and 20%. (d) is the relationship between internal resistance and NaCl concentration, (e) is the EIS spectra of MFCs in difference NaCl concentrations, and (f) is the relationship between charge transfer and solution resistance to internal resistance.

### 3.1.3 Application on fish processing wastewater

To evaluate the biodegradability of *B. clausii* J1G-0%B, we investigated the Chemical Oxygen Demand (COD) of fish processing wastewater collected from a local fish processing factory in Semarang, Indonesia. The analysis was conducted before and after treatment using Microbial Fuel Cells (MFCs). Table 3 displays the properties of fish processing effluent before and after treatment with and without *B. clausii*. The average values for chemical oxygen demand (COD)

and salinity in fish processing wastewater were  $14750 \pm 375$  ppm and  $6.1 \pm 0.3$  %, respectively. Following the introduction of *B. clausii* treatment in MFCs, a significant decrease in COD levels was noticed. The estimated COD removal efficiency was measured at  $95.45 \pm 1.07$  %, reducing the levels from  $14750 \pm 375$  to  $674 \pm 14$  ppm. The significant reduction in COD after treatment with MFCs highlights the notion of microbial remediation. Meanwhile, a decrease also occurred in the MFC system without the presence of halophilic bacteria, but it was not significant from



14750 ± 375 to 11385 ± 247, or only 23%. This decrease in COD may be due to the activity of bacterial consortia that have been present in seafood processing wastewater since the beginning. This result is comparable to or even better than previous halophilic MFCs as shown in Table 3 [6], [9], [11], [13], [56]–[58]. Microorganisms, led by the biocatalyst *B. clausii*, participate in a coordinated metabolic process to break down and absorb organic contaminants. This mechanism is consistent with the microbial degradation hypothesis, which states that bacteria use organic chemicals as sources of energy, transforming them into biomass, gasses, and simpler, less toxic substances. The COD, which measures the amount of oxygen needed for chemical oxidation, significantly decreases as a result. This decrease indicates the effective conversion of complicated contaminants into environmentally friendly forms via the activities of microbial enzymes. In addition, the pH of wastewater rises from 6.88 ± 0.13 to 8.38 ± 0.38. The increase in pH after treatment indicates the strong microbial ability inside the MFC system. During the process of metabolizing organic acids, bacteria generate a significant number of alkaline byproducts, such as ammonia or bicarbonate ions. The use of *B. clausii* as a biocatalyst leads to a significant change towards a more alkaline environment via biochemical reactions. The decomposition of organic compounds has the dual purpose of purifying the effluent from seafood processing and increasing the pH levels. This event highlights the efficacy of microbial fuel cells in facilitating transformational processes, resulting in treated water that is more favorable for environmental well-being and safety. The total dissolved solids (TDS) in the wastewater increased by 18.3% from 4057 ± 24 to 4800 ± 37 ppm. Microbial metabolism can lead to the release of byproducts or metabolic intermediates into the treated water, contributing to the observed increase in TDS. *B. clausii*, often produces extracellular polymeric substances (EPS) as part of

their biofilm formation. EPS can contribute to the TDS in the wastewater as they contain organic and inorganic components. Moreover, the treatment process may involve the breakdown and mineralization of organic compounds present in fish processing wastewater. This breakdown can result in the release of inorganic ions and contribute to the overall TDS of the water. The ORP value has increased from -177 ± 11 to -7 ± 0.2 mV. The increase in ORP after treatment reveals the complex redox dynamics controlled by MFCs. Microorganisms inside the MFC system operate as catalysts for electron transfer, facilitating redox processes. Based on the idea of microbial fuel cells, this increase in ORP indicates a transition towards a more oxidized condition. Microbes efficiently utilize electron donors in fish processing wastewater, demonstrating their crucial function as primary agents in oxidative reactions. The rise in ORP serves as evidence of the effectiveness of MFCs in using microbial activities to facilitate oxidation, which is essential for the efficient elimination and conversion of contaminants in fish processing wastewater. The salinity and temperature undergo insignificantly changes from 6.1 ± 0.3 to 6.0 ± 0.1% and 24 ± 2 to 29 ± 1.4 °C, respectively, throughout the incubation period. *B. clausii* undergoes metabolic processes during incubation. Microbial metabolism involves the breakdown of organic matter, which can be exothermic. Furthermore, the concentration of dissolved H<sub>2</sub> increases from 0.36 ± 0.07 to 0.02 ± 0.00 ppm. The decrease in dissolved hydrogen concentration may indicate that the microorganisms, including *B. clausii*, are effectively utilizing the hydrogen produced during the treatment process for their metabolic activities. On the other hand, The MFC system might be facilitating efficient electron transfer during the microbial degradation of organic compounds in the wastewater, resulting in the observed decrease in dissolved hydrogen concentration.

**Table 3:** COD removal comparison of wastewater using MFCs.

Biocatalyst	Substrate	MFC System	COD Removal (%)	Ref.
Halophilic consortium bacteria	seafood industrial wastewater	single chamber	85	[58]
Halophilic consortium bacteria	fish market wastewater	single chamber	84	[8]
Halophilic consortium bacteria	tannery wastewater	single chamber	93	[13]
Halophilic consortium bacteria	aquaculture wastewater	double chamber	92	[11]
<i>H. praevalens</i> and <i>M. hydrocarbonoclasticus</i>	Barnett Shale produced water	single chamber	68	[59]
Halophilic consortium bacteria	pharmaceutical industrial wastewater	single chamber	92	[58]
<i>B. clausii</i>	fish processing wastewater	single chamber	95.45	this work

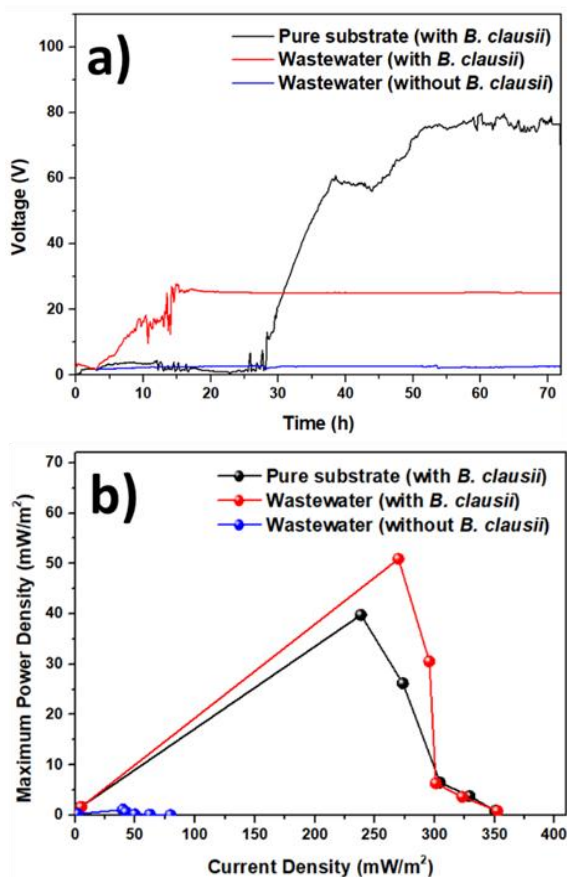


**Figure 8:** (a) Voltage and (b) power curves of halophilic bacteria MFCs in NaCl level of 10% compared to real fish processing wastewater as substrate on one cycle.

In bioelectricity production, the voltage attained by MFC using wastewater substrate may approach  $26.15 \pm 1.84$  mV, which is lower than that achieved when using a pure substrate (halophilic medium only) as shown in Figure 8(a). While, the average voltage of MFCs using wastewater only, without halophilic bacteria were  $2.94 \pm 0.32$  mV, respectively. Pure substrates typically have a simpler and more readily available energy source for microorganisms. In wastewater, the organic content is often complex and may require a series of microbial reactions to break down into simpler compounds before it can be used for energy production. This complexity can result in a slower and less efficient electron transfer process, leading to lower voltage. Moreover, wastewater often contains various impurities and inhibitors that can affect microbial activity and hinder electron transfer reactions. These inhibitors may include heavy metals,

toxins, or other compounds that can interfere with microbial metabolism and reduce the overall efficiency of the MFC. *B. clausii* in MFCs with pure substrates may be specifically adapted to utilize that particular substrate, leading to a more efficient and rapid electron transfer process. In contrast, *B. clausii* in wastewater-fed MFCs may need time to adapt to the varying composition of the wastewater, affecting the overall performance. Surprisingly, the power curves demonstrate a special trend in the case of MPD, whereby halophilic MFCs using fish processing wastewater as a substrate have a higher MPD value in comparison to the pure substrate, which the results were  $50.92 \pm 0.28$  mW/m<sup>2</sup> or 31% higher (Figure 8(b)). While the power resulted by MFCs using fish processing wastewater without halophilic bacteria was  $1.11 \pm 0.04$  mW/m<sup>2</sup>. Despite the higher output voltage, the MPD of pure substrate-fed halophilic MFCs might be lower due to some limitations, such as nutrient scarcity, electron donor availability, or metabolic pathway differences.

### 3.2 Investigation of biofilm formation

Changes in dry weight on the electrode are used to indicate the biofilm formed. Dry weight measurements were carried out before and after incubation for  $3 \times 72$  h. The SEM pictures in Figure 9(a) show plain carbon felt without any bacterial growth on its surface. Figure 9(b) depicts the growth of halophilic bacteria on the surface of CF without the addition of NaCl. In the absence of sodium chloride (NaCl), the growth of halophilic bacteria exhibited non-uniformity. Bacterial growth would occur only in certain areas. In contrast to Figure 9(c), where the growth of halophilic bacteria was supported by the addition of 10% NaCl. The halophilic bacteria exhibit enhanced growth and more uniformity when cultivated on the surface of CF. Figure 9(d) is the weight and photograph of biofilm attached to the surface of the anode, confirming that the weight of biofilm has a positive correlation with the MPD of MFCs. A discernible deposit with a substantial and organized structure is seen on the water-facing surface of the anode. The formation of these deposits may be attributed to the growth of biofilms, as well as the accumulation of various substances resulting from variations in salt levels [60]. With a NaCl of 10% compared to the other samples, it can be shown that the halophilic bacteria adhered to the carbon felt fibers in the MFC were qualitatively the most halophilic

bacteria. This finding aligns with the outcomes obtained from the electrochemical analysis conducted on both the half-cell and full-cell configurations. The growth of biofilms on the electrodes is influenced by the concentration of salinity [61]. The growth of biofilms plays a crucial role in facilitating the generation of energy using MFCs. The data from measuring the biofilm weight reveals a direct correlation between biofilm weight and the performance of MFCs. This relationship is attributed to the involvement of bacteria in metabolic processes, leading to the production of protons and electrons. Surprisingly, an anomaly is observed in the

comparison between biofilm weights at 15% NaCl and 10% NaCl concentrations. Despite the MFC performance suggesting otherwise, the biofilm weight at 15% NaCl appears slightly greater than at 10% NaCl. This discrepancy implies that the measured biofilm weight does not solely represent a thriving and metabolically active biofilm. Instead, it seems to include debris from bacteria that have undergone lysis or maybe salt crystal. This distinction is crucial as it suggests that the recorded biofilm weight may not accurately reflect the live and metabolizing biofilm contributing to the production of protons and electrons in the MFCs [62].

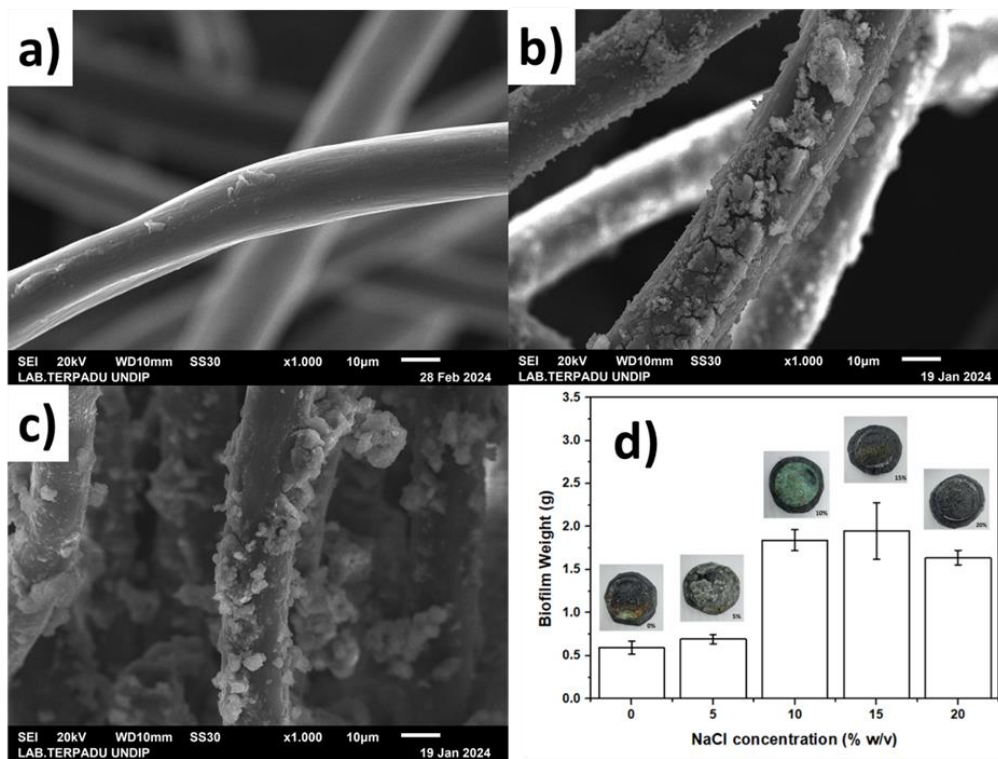


**Figure 9:** The SEM image of (a) plain CF, (b) halophilic bacteria biofilm without NaCl and (c) with 10% NaCl. While (d) biofilm weight attached to the surface of the anode with its photograph.

### 3.3 Tryptone metabolism mechanism in *B. clausii*

Tryptone pathway metabolism by *B. clausii* is presented because previously there has not been a complete explanation regarding the consumption of tryptone until the release of electrons from the cells. Tryptone is a polypeptide derived from the hydrolysis process of casein, containing several amino acids, with

tryptophan being the most abundant [63]. In the bacterial metabolism of *B. clausii* J1G-0%B, tryptone undergoes hydrolysis, including tryptophan and other amino acids, facilitated by the enzyme trypsin [64]. The produced tryptophan is transported into the cell towards the cytoplasm. Inside the cytoplasm, tryptophan undergoes hydrolysis with the help of the enzyme tryptophanase, resulting in indole and alanine.



Alanine transfers its amino group to  $\alpha$ -ketoglutarate, forming glutarate and pyruvate, with ammonia as a byproduct [65]. Pyruvate is then converted to acetyl-CoA, releasing one carbon as carbon dioxide, and the remaining two carbons combine with coenzyme A (CoA) to form acetyl-CoA and activate NADH from  $\text{NAD}^+$ . The generated acetyl-CoA from the conversion of pyruvate enters the Krebs cycle (TCA cycle). In the Krebs cycle, acetyl-CoA combines with oxaloacetate to form citrate, initiating a series of oxidative reactions that produce energy through ATP production, as well as activating NADH from  $\text{NAD}^+$  and  $\text{FADH}_2$  from FAD [66].

Tryptophan, an essential amino acid, can contribute to the formation of  $\text{NAD}^+$  through the kynurenine pathway [67]. This metabolic pathway involves the enzymatic breakdown of tryptophan's aromatic ring, initiated by the action of the enzyme tryptophan-2,3-dioxygenase (TDO) or indoleamine 2,3-dioxygenase (IDO). These enzymes convert tryptophan into N-formylkynurenine. The process commences with the hydrolysis of tryptophan's aromatic ring by TDO or IDO, resulting in the formation of N-formylkynurenine. Subsequently, N-formylkynurenine undergoes a conversion process, wherein the formyl group is removed to produce kynurenine. Kynurenine then undergoes further transformations, ultimately leading to the formation of 3-hydroxykynurenine. The kynurenine pathway diverges at this point. One branch contributes to the synthesis of quinolinic acid, a precursor of  $\text{NAD}^+$ . In this branch, 3-hydroxykynurenine serves as a precursor, and through a series of reactions, quinolinic acid is eventually formed. Simultaneously, an alternative branch involves 3-hydroxykynurenine undergoing a distinct series of reactions, culminating in the formation of 2-aminomuconic acid. This compound is then converted to glutamyl-CoA, and subsequently, it enters the Krebs cycle after being converted into acetyl-CoA. This part of the pathway allows tryptophan to contribute to energy production through its integration into the Krebs cycle.

The Krebs cycle begins with citric acid produced from the reaction between oxaloacetate and acetyl-CoA. Through a series of oxidative and electron transfer reactions, citric acid gradually undergoes decarboxylation, producing  $\text{CO}_2$ . Each stage generates an intermediate compound, which then reacts to form the next cycle compound. During this process, acetyl-CoA molecules are transformed into three NADH molecules, one  $\text{FADH}_2$  molecule, and one GTP

molecule (equivalent to ATP). After the TCA cycle, NADH and  $\text{FADH}_2$  carry electrons to the Electron Transport Chain (ETC) within the inner cell membrane. Complexes I, II, and III in the ETC receive and transfer electrons, producing energy used to pump protons into the intermembrane space. Electrons then exit the inner cell membrane and then to the electrode, contributing to extracellular electron transfer flow. Thus, the Krebs cycle and the Electron Transport Chain collaboratively eliminate carbon dioxide and produce electron carrier molecules that provide energy to establish an electrochemical gradient.

#### 4 Conclusions

In unraveling the electrochemical intricacies of halophilic bacterial MFCs under varying NaCl concentrations, this study illuminates the unique potential of *B. clausii* in saline environments. The fish industry wastewater has not yet been effectively treated, and MFCs present a viable solution. Halophilic bacteria, such as *B. clausii*, can be effectively used as biocatalysts due to their ability to thrive in high salinity levels present in such wastewater. Halophiles' metabolic prowess is seen by the oxidation peak at  $-0.75$  V vs. Ag/AgCl, which reduces  $\text{NAD}^+$  to NADH. The lack of oxidation peaks under certain circumstances suggests the bacterium struggles with salt adaption, osmotic balance, and nutrient absorption. *B. clausii* metabolism increases at 10% NaCl, preventing osmotic stress and retaining salt adaption. The subtle influence on reduction and oxidation processes emphasizes the delicate balance needed for efficient electrogenic function. Cyclic voltammetry profiles focus on NaCl concentration to optimize electrode and biocatalyst development. The electron transfer rate constant ( $k_s$ ) is a crucial metric, peaking at 10% NaCl concentration ( $2.318 \pm 0.037 \text{ s}^{-1}$ ). Salinity facilitates electron transport, which is crucial for microbial fuel cell redox processes. *B. clausii* J1G-0%B is a better biocatalyst with higher  $k_s$  values than prior investigations. In fish processing wastewater treatment, *B. clausii* achieves  $95.45 \pm 1.07\%$  COD removal efficiency at 10% NaCl concentration and a significant increase in MPD up to  $50.92 \pm 0.28 \text{ mW/m}^2$ . The research suggests this strain is a potential and eco-friendly biocatalyst for saline wastewater treatment. In conclusion, this study illuminates halophilic bacterial MFCs' electrochemical properties and highlights *B. clausii* biocatalytic versatility. The results help optimize microbial fuel cells in saline

conditions for sustainable industrial wastewater treatment and bioelectricity production.

Utilizing halophilic bacteria as MFC biocatalysts to treat fish industry wastewater can significantly reduce contamination, making the process environmentally friendly. Additionally, this approach can generate electricity, providing a dual benefit of waste treatment and energy production. It is anticipated that the treatment using halophilic MFCs will be more cost-effective than conventional methods. This expectation is based on the dual functionality of waste treatment and electricity generation, which could offset operational costs.

### Acknowledgments

This research fully funded by Director of Research, Technology and Community Service - Ministry of Education, Culture, Research, and Technology through Regular Fundamental Research scheme (No. 449A-31/UN7.D2/PP/VI/2023).

### Author Contributions

M.C.: funding acquisition, conceptualization, methodology, writing an original draft; reviewing and editing; M.R.S.: investigation, data analysis; M.A.: conceptualization, research design; H.H.: data curation, writing—reviewing and editing, project administration. All authors have read and agreed to the published version of the manuscript.

### Conflicts of Interest

The authors declare that they have no known competing financial interests or personal relationships that could have appeared to influence the work reported in this paper.

### References

- [1] H. T. H. Anh, E. Shahsavari, N. J. Bott, and A. S. Ball, "Options for improved treatment of saline wastewater from fish and shellfish processing," *Frontiers in Environmental Science*, vol. 9, pp. 1–16, 2021.
- [2] J. V. Boas, V. B. Oliveira, M. Simões, and A. M. Pinto, "Review on microbial fuel cells applications, developments and costs," *Journal of Environmental Management*, vol. 307, pp. 1–19, 2022.
- [3] K., Obileke, H. Onyeaka, E. L. Meyer, and N. Nwokolo, "Microbial fuel cells, a renewable energy technology for bio-electricity generation: A mini-review," *Electrochemistry Communications*, vol. 125, pp. 1–14, 2021.
- [4] M. Grattieri and S. D. Minteer, "Microbial fuel cells in saline and hypersaline environments: Advancements, challenges and future perspectives," *Bioelectrochemistry*, vol. 120, pp. 127–137, 2018.
- [5] I. M. Simeon, A. Weig, and R. Freitag, "Optimization of soil microbial fuel cell for sustainable bio-electricity production: combined effects of electrode material, electrode spacing, and substrate feeding frequency on power generation and microbial community diversity," *Biotechnology for Biofuels and Bioproducts*, vol. 15, no. 124, pp. 1–19, 2022.
- [6] F. Guo, H. Luo, Z. Shi, Y. Wu, and H. Liu, "Substrate salinity: a critical factor regulating the performance of microbial fuel cells, a review," *Science of The Total Environment*, vol. 763, pp. 1–16, 2021.
- [7] S. J. Robertson, M. Grattieri, J. Behring, M. Bestetti, and S. D. Minteer, "Transitioning from batch to flow hypersaline microbial fuel cells," *Electrochimica Acta*, vol. 317, pp. 494–501, 2019.
- [8] M. T. Jamal and A. Pugazhendi, "Treatment of fish market wastewater and energy production using halophiles in air cathode microbial fuel cell," *Journal of Environmental Management*, vol. 292, pp. 1–7, 2021.
- [9] B. Zhang and Z. He, "Improving water desalination by hydraulically coupling an osmotic microbial fuel cell with a microbial desalination cell," *Journal of Membrane Science*, vol. 441, pp. 18–24, 2013.
- [10] J. Qiu, R. Han, and C. Wang, "Microbial halophilic lipases: A review," *Journal of Basic Microbiology*, vol. 61, no. 7, pp. 594–602, 2021.
- [11] A. Pugazhendi, G. G. Alreeshi, M. T. Jamal, T. Karuppiah, and R. B. Jeyakumar, "Bioenergy production and treatment of aquaculture wastewater using saline anode microbial fuel cell under saline condition," *Environmental Technology & Innovation*, vol. 21, pp. 1–9, 2021.
- [12] W. Liu and Y. Wu, "Simultaneous nitrification, denitrification and electricity recovery of *halomonas* strains in single chamber microbial fuel cells for seawater sewage treatment,"





- Journal of Environmental Chemical Engineering*, vol. 9, no. 6, pp. 1–8, 2021.
- [13] R. E. A. Ghorab, A. Pugazhendi, M. T. Jamal, R. B. Jeyakumar, J. J. Godon, and D. K. Mathew, “Tannery wastewater treatment coupled with bioenergy production in upflow microbial fuel cell under saline condition,” *Environmental Research*, vol. 212, pp. 1–7, 2022.
- [14] R. Gurav, S. K. Bhatia, T. R. Choi, H. R. Jung, S. Y. Yang, H. S. Song, Y. L. Park, Y. H. Han, J. Y. Park, Y. G. Kim, K. Y. Choi and Y. H. Yang, “Chitin biomass powered microbial fuel cell for electricity production using halophilic *Bacillus circulans* bbl03 isolated from sea salt harvesting area,” *Bioelectrochemistry*, vol. 130, pp. 1–8, 2019.
- [15] O. Monzon, Y. Yang, Q. Li, and P. J. Alvarez, “Quorum sensing autoinducers enhance biofilm formation and power production in a hypersaline microbial fuel cell,” *Biochemical Engineering Journal*, vol. 109, pp. 222–227, 2016.
- [16] E. Ghelardi, A. T. Abreu y Abreu, C. B. Marzet, G. Álvarez Calatayud, M. Perez III, and A. P. Moschione Castro, “Current progress and future perspectives on the use of *Bacillus clausii*,” *Microorganisms*, vol. 10, no. 6, pp. 1–16, 2022.
- [17] L. Muschallik, D. Molinnus, J. Bongaerts, M. Pohl, T. Wagner, M. J. Schöning, P. Siegert, and T. Selmer, “(r, r)-butane-2, 3-diol dehydrogenase from *B. clausii* dsm 8716t, cloning and expression of the *bdhA*-gene, and initial characterization of enzyme,” *Journal of Biotechnology*, vol. 258, pp. 41–50, 2017.
- [18] G. D. Arum, M. Asy'ari, and N. S. Mulyani, “Effect of storage of yellow pigment from Halophilic *Bacillus clausii* J1G-0%B on antioxidant activity,” *Jurnal Kimia Sains dan Aplikasi*, vol. 25, no. 11, pp. 399–404, 2022.
- [19] M. Christwardana, D. Frattini, G. Accardo, S. P. Yoon, and Y. Kwon, “Early-stage performance evaluation of flowing microbial fuel cells using chemically treated carbon felt and yeast biocatalyst,” *Applied Energy*, vol. 222, pp. 369–382, 2018.
- [20] M. Christwardana, D. Frattini, G. Accardo, S. P. Yoon, and Y. Kwon, “Effects of methylene blue and methyl red mediators on performance of yeast based microbial fuel cells adopting polyethylenimine coated carbon felt as anode,” *Journal of Power Sources*, vol. 396, pp. 1–11, 2018.
- [21] M. Christwardana, D. Frattini, G. Accardo, S. P. Yoon, and Y. Kwon, “Optimization of glucose concentration and glucose/yeast ratio in yeast microbial fuel cell using response surface methodology approach,” *Journal of Power Sources*, vol. 402, pp. 402–412, 2018.
- [22] M. Christwardana, J. Joelianingsih, and L. A. Yoshi, “A novel of 2d-3d combination carbon electrode to improve yeast microbial fuel cell performance,” *Journal of Applied Electrochemistry*, vol. 52, pp. 801–812, 2022.
- [23] M. Christwardana, J. Joelianingsih, L. A. Yoshi, and H. Hadiyanto, “Binderless carbon nanotube/carbon felt anode to improve yeast microbial fuel cell performance,” *Current Research in Green and Sustainable Chemistry*, vol. 5, pp. 1–11, 2022.
- [24] Y. H. Chen, C. W. Lu, Y. T. Shyu, and S. S. Lin, “Revealing the saline adaptation strategies of the halophilic bacterium *Halomonas beimenensis* through high-throughput omics and transposon mutagenesis approaches,” *Scientific Reports*, vol. 7, pp. 1–15, 2017.
- [25] C. Kumawat, A. Kumar, J. Parshad, S. S. Sharma, A. Patra, P. Dogra, G. K. Yadav, S. K. Dadhich, R. Verma and G. L. Kumawat, “Microbial diversity and adaptation under salt-affected soils: A review,” *Sustainability*, vol. 14, no. 15, pp. 1–24, 2022.
- [26] A. Vijay, P. C. Ghosh, and S. Mukherji, “Power generation by halophilic bacteria and assessment of the effect of salinity on performance of a denitrifying microbial fuel cell,” *Energies*, vol. 16, no. 2, pp. 1–16, 2023.
- [27] M. Hemalatha, J. S. Sravan, and S. V. Mohan, “Self-induced bioelectro-potential influence on sulfate removal and desalination in microbial fuel cell,” *Bioresource Technology*, vol. 309, pp. 1–9, 2020.
- [28] F. Orhan, “Potential of halophilic/halotolerant bacteria in enhancing plant growth under salt stress,” *Current Microbiology*, vol. 78, pp. 3708–3719, 2021.
- [29] I. P. Guynn, K. Beaver, E. M. Gaffney, A. B. Zani, A. Dantanarayana, and S. D. Minter, “*Salinivibrio* sp. eagsl as a halophilic and ectoine-producing bacteria for broad microbial electrochemistry applications,” *Cell Reports Physical Science*, vol. 4, no. 6, pp. 1–11, 2023.

- [30] J. F. Rusling and S. L. Suib, "Characterizing materials with cyclic voltammetry," *Advanced Materials*, vol. 6, no. 12, pp. 922–930, 1994.
- [31] M. Yang, Y. Zhong, J. Ren, X. Zhou, J. Wei, and Z. Zhou, "Fabrication of high-power Li-ion hybrid supercapacitors by enhancing the exterior surface charge storage," *Advanced Energy Materials*, vol. 5, no. 17, pp. 1–7, 2015.
- [32] S. Sevda, K. Chayambuka, T. R. Sreekrishnan, D. Pant, and X. Dominguez-Benetton, "A comprehensive impedance journey to continuous microbial fuel cells," *Bioelectrochemistry*, vol. 106, pp. 159–166, 2015.
- [33] K. Kim, D. Hwang, S. Kim, S. O. Park, H. Cha, Y. S. Lee, J. Cho, S. K. Kwak and N. S. Choi, "Cyclic aminosilane-based additive ensuring stable electrode–electrolyte interfaces in Li-ion batteries," *Advanced Energy Materials*, vol. 10, no. 15, pp. 1–12, 2020.
- [34] E. Laviron, "General expression of the linear potential sweep voltammogram in the case of diffusionless electrochemical systems," *Journal of Electroanalytical Chemistry and Interfacial Electrochemistry*, vol. 101, no. 1, pp. 19–28, 1979.
- [35] X. W. Liu, Y. X. Huang, X. F. Sun, G. P. Sheng, F. Zhao, S. G. Wang, and H. Q. Yu, "Conductive carbon nanotube hydrogel as a bioanode for enhanced microbial electrocatalysis," *ACS Applied Materials & Interfaces*, vol. 6, no. 11, pp. 8158–8164, 2014.
- [36] M. Shabani, M. Ponti, H. Younesi, M. Nacef, A. Rahimpour, M. Rahimnejad, and R. M. Bouchenak Khelladi, "Biodegradation of acetaminophen and its main by-product 4-aminophenol by *trichoderma harzianum* versus mixed biofilm of *trichoderma harzianum/pseudomonas fluorescens* in a fungal microbial fuel cell," *Journal of Applied Electrochemistry*, vol. 51, pp. 581–596, 2021.
- [37] L. Huang, X. Zhang, D. Shen, N. Li, Z. Ge, Y. Zhou, M. Zhou, H. Feng and K. Guo, "Effect of heat-treatment atmosphere on the current generation of TiO<sub>2</sub> nanotube array electrodes in microbial fuel cells," *Electrochimica Acta*, vol. 257, pp. 203–209, 2017.
- [38] Y. Wang, Q. Wen, Y. Chen, and W. Li, "Conductive polypyrrole-carboxymethyl cellulose-titanium nitride/carbon brush hydrogels as bioanodes for enhanced energy output in microbial fuel cells," *Energy*, vol. 204, pp. 1–12, 2020.
- [39] Y. Chen, Z. Zhao, S. Li, B. Li, Z. Weng, Y. Fang, W. Lei, and H. Jiang, "Fabrication of 3D graphene anode for improving performance of miniaturized microbial fuel cells," *3 Biotech*, vol. 12, pp. 1–10, 2022.
- [40] M. Asghary, J. B. Raoof, M. Rahimnejad, and R. Ojani, "Microbial fuel cell-based self-powered biosensing platform for determination of ketamine as an anesthesia drug in clinical serum samples," *Journal of the Iranian Chemical Society*, vol. 15, pp. 445–453, 2018.
- [41] T. Christiansen and J. Nielsen, "Growth energetics of an alkaline serine protease-producing strain of *b. clausii* during continuous cultivation," *Bioprocess and Biosystems Engineering*, vol. 24, pp. 329–339, 2002.
- [42] A. K. Prabowo, A. P. Tiarasukma, M. Christwardana, and D. Ariyanti, "Microbial fuel cells for simultaneous electricity generation and organic degradation from slaughterhouse wastewater," *International Journal of Renewable Energy Development*, vol. 5, no. 2, pp. 107–112, 2016.
- [43] F. Xing, H. Xi, Y. Yu, and Y. Zhou, "Anode biofilm influence on the toxic response of microbial fuel cells under different operating conditions," *Science of The Total Environment*, vol. 775, pp. 1–8, 2021.
- [44] P. Xu, E. Xiao, L. Zeng, F. He, and Z. Wu, "Enhanced degradation of pyrene and phenanthrene in sediments through synergistic interactions between microbial fuel cells and submerged macrophyte *vallisneria spiralis*," *Journal of Soils and Sediments*, vol. 19, pp. 2634–2649, 2019.
- [45] R. Karthikeyan, A. Selvam, K. Y. Cheng, and J. W. C. Wong, "Influence of ionic conductivity in bioelectricity production from saline domestic sewage sludge in microbial fuel cells," *Bioresour. Technology*, vol. 200, pp. 845–852, 2016.
- [46] A. Vijay, S. Arora, S. Gupta, and M. Chhabra, "Halophilic starch degrading bacteria isolated from sambhar lake, India, as potential anode catalyst in microbial fuel cell: A promising process for saline water treatment," *Bioresour. Technology*, vol. 256, pp. 391–398, 2018.
- [47] R. Gurav, S. K. Bhatia, T. R. Choi, H. R. Jung, S. Y. Yang, H. S. Song, Y. L. Park, Y. H. Han, J. Y.



- Park, Y. G. Kim, K. Y. Choi, and Y. H. Yang, "Chitin biomass powered microbial fuel cell for electricity production using halophilic *bacillus circulans* bbl03 isolated from sea salt harvesting area," *Bioelectrochemistry*, vol. 130, pp. 1–8, 2019.
- [48] B. R. Sreelekshmy, R. Basheer, and S. M. A. Shibli, "Exploration of bifurcated electron transfer mechanism in *bacillus cereus* for enhanced power generation in double-chambered microbial fuel cells," *Journal of Environmental Chemical Engineering*, vol. 10, no. 3, pp. 1–13 2022.
- [49] V. R. Nimje, C. Y. Chen, C. C. Chen, J. S. Jean, A. S. Reddy, C. W. Fan, K. Y. Pan, H. T. Liu, and J. L. Chen, "Stable and high energy generation by a strain of *bacillus subtilis* in a microbial fuel cell," *Journal of Power Sources*, vol. 190, no. 2, pp. 258–263, 2009.
- [50] A. Dongre, R. K. Sharma, M. Sogani, and N. K. Poddar, "Ultrasonic pre-treatment of *bacillus velezensis* for improved electrogenic response in a single chambered microbial fuel cell," *3 Biotech*, vol. 12, pp. 1–12, 2022.
- [51] Y. C. Yong, Z. H. Liao, J. Z. Sun, T. Zheng, R. R. Jiang, and H. Song, "Enhancement of coulombic efficiency and salt tolerance in microbial fuel cells by graphite/alginate granules immobilization of *shewanella oneidensis* mr-1," *Process Biochemistry*, vol. 48, no. 12, pp. 1947–1951, 2013.
- [52] P. Srimuk, X. Su, J. Yoon, D. Aurbach, and V. Presser, "Charge-transfer materials for electrochemical water desalination, ion separation and the recovery of elements," *Nature Reviews Materials*, vol. 5, pp. 517–538, 2020.
- [53] J. Wang, Y. Liu, Y. Ma, X. Wang, B. Zhang, G. Zhang, A. Bahadur, T. Chen, G. Liu, W. Zhang, and Y. Zhao, "Research progress regarding the role of halophilic and halotolerant microorganisms in the eco-environmental sustainability and conservation," *Journal of Cleaner Production*, vol. 418, pp. 1–13, 2023.
- [54] F. Wu, W. Li, L. Chen, Y. Su, L. Bao, W. Bao, Z. Yang, J. Wang, Y. Lu and S. Chen, "Renovating the electrode-electrolyte interphase for layered lithium-& manganese-rich oxides," *Energy Storage Materials*, vol. 28, pp. 383–392, 2020.
- [55] B. Kim, I. S. Chang, R. M. Dinsdale, and A. J. Guwy, "Accurate measurement of internal resistance in microbial fuel cells by improved scanning electrochemical impedance spectroscopy," *Electrochimica Acta*, vol. 366, pp. 1–30, 2021.
- [56] T. Liu, Y. Y. Yu, D. Li, H. Song, X. Yan, and W. N. Chen, "The effect of external resistance on biofilm formation and internal resistance in shewanella inoculated microbial fuel cells," *RSC Advances*, vol. 6, no. 24, pp. 1–19, 2016.
- [57] T. Cai, Y. Zhang, N. Wang, Z. Zhang, X. Lu, and G. Zhen, "Electrochemically active microorganisms sense charge transfer resistance for regulating biofilm electroactivity, spatio-temporal distribution, and catabolic pathway," *Chemical Engineering Journal*, vol. 442, pp. 1–12, 2022.
- [58] M. T. Jamal, A. Pugazhendi, and R. B. Jeyakumar, "Application of halophiles in air cathode MFC for seafood industrial wastewater treatment and energy production under high saline condition," *Environmental Technology & Innovation*, vol. 20, pp. 1–11, 2020.
- [59] O. Monzon, Y. Yang, J. Kim, A. Heldenbrand, Q. Li, and P. J. Alvarez, "Microbial fuel cell fed by barnett shale produced water: power production by hypersaline autochthonous bacteria and coupling to a desalination unit," *Biochemical Engineering Journal*, vol. 117, pp. 87–91, 2017.
- [60] A. Pugazhendi, M. T. Jamal, B. A. Al-Mur, and R. B. Jeyakumar, "Bioaugmentation of electrogenic halophiles in the treatment of pharmaceutical industrial wastewater and energy production in microbial fuel cell under saline condition," *Chemosphere*, vol. 288, pp. 1–9, 2022.
- [61] M. Grattieri, M. Suvira, K. Hasan, and S. D. Minter, "Halotolerant extremophile bacteria from the great salt lake for recycling pollutants in microbial fuel cells," *Journal of Power Sources*, vol. 356, pp. 310–318, 2017.
- [62] M. Christwardana, G. E. Timuda, N. Darsono, H. Widodo, K. Kurniawan, and D. S. Khaerudini, "Fabrication of a polyvinyl alcohol-bentonite composite coated on a carbon felt anode for improving yeast microbial fuel cell performance," *Journal of Power Sources*, vol. 555, pp. 1–9, 2023.
- [63] A. Mishra and M. Chhabra, "Performance of photo-microbial fuel cell with *Dunaliella salina* at the saline cathode," *Bioresource Technology Reports*, vol. 19, pp. 1–8, 2022.
- [64] M. Puhm, H. Ainelo, M. Kivisaar, and R. Teras, "Tryptone in growth media enhances *pseudomonas*



- putida* biofilm,” *Microorganisms*, vol. 10, no. 3, pp. 1–19, 2022.
- [65] T. Teraishi, H. Hori, D. Sasayama, J. Matsuo, S. Ogawa, M. Ota, K. Hattori, M. Kajiwara, T. Higuchi, and H. Kunugi “<sup>13</sup>C-tryptophan breath test detects increased catabolic turnover of tryptophan along the kynurenine pathway in patients with major depressive disorder,” *Scientific Reports*, vol. 5, pp. 1–10, 2015.
- [66] E. A. C. Hababag, A. Cauilan, D. Quintero, and D. Bermudes, “Tryptophanase expressed by *salmonella* halts breast cancer cell growth in vitro and inhibits production of immunosuppressive kynurenine,” *Microorganisms*, vol. 11, no. 5, pp. 1–14, 2023.
- [67] A. P. Jiménez-Urbe, E. Y. Hernández-Cruz, K. J. Ramírez-Magaña, and J. Pedraza-Chaverri, “Involvement of tricarboxylic acid cycle metabolites in kidney diseases,” *Biomolecules*, vol. 11, no. 9, pp. 1–20, 2021.